

Multiscale Voter Model on Real Networks

Elisenda Ortiz^{1,2} and M. Ángeles Serrano^{1,2,3,*}

¹*Departament de Física de la Matèria Condensada,*

Universitat de Barcelona, Martí i Franquès 1, 08028 Barcelona, Spain

²*Universitat de Barcelona Institute of Complex Systems (UBICS), Universitat de Barcelona, Barcelona, Spain*

³*ICREA, Pg. Lluís Companys 23, E-08010 Barcelona, Spain*

(Dated: June 2, 2022)

We introduce the Multiscale Voter Model (MVM) to investigate clan influence at multiple scales in opinion formation on complex networks. We run numerical simulations to monitor the evolution of MVM dynamics in real and synthetic networks, and identified a transition between a final stage of full consensus and one with mixed binary opinions. The transition depends on the scale of the clans—made of similar nodes detected in network embeddings—and on the strength of their influence. We found that enhancing group diversity promotes consensus while strong kinship yields to metastable clusters of same opinion. The segregated domains, which signal opinion polarization, are discernible as spatial patterns in the hyperbolic embeddings of the networks. Our multiscale framework can be easily exported to other dynamical processes affected by scale and group influence.

Opinion dynamics can be modeled using interacting agents in social networks in order to investigate the spreading of attitudes, beliefs, and sentiments in society. In this context, the Voter Model (VM) is an archetypal stochastic nonequilibrium model that gives a standard framework for studying imitation as an underlying mechanism of opinion formation [1, 2]. In networks, the small-world property reduces extremely the time to reach consensus in finite systems [3, 4], and heterogeneous distributions of the number of neighbors also promote quick agreement [5]. Conversely, in real life scenarios we rarely find a large group of individuals easily coming to a consensus on sensitive topics. This dichotomy has motivated generalizations of the VM that include more realistic features such as zealots, bounded confidence, noise or memory effects [6].

Here, we address this contradiction by introducing the Multiscale Voter Model (MVM), which assumes the decisions of an individual are affected by the viewpoint of its own group. Despite group-level information is known to affect behavioural responses in human [7] and even in animal [8] social networks, few models account for it. Among them, there is the q -voter model [9] where an agent takes the opinion of q connected neighbors that agree, the majority-vote model [10] where a node copies the state of the majority of its neighbors, and other models that introduce similar types of non-linearities [11]. Other alternatives use multiplex network representations [12, 13], or couple individual information exchange with external information fields [14]. Instead, the MVM relies on the geometric embedding of a network [15] to define clans of similar nodes (not necessarily neighbors) at some specific granularity—family, neighborhood, political party, country—that influence the decision of copying a neighbor. The model interpolates in a natural way between states that reach consensus fast,

as in the VM in small-world networks, and frozen disordered states typical of lattices, going through competition between opinion domains.

Each node i in the MVM holds one of two possible opinions $s_i = \{-1, 1\}$, and nodes interact by copying the state of a randomly chosen neighbor. To avoid biases induced by heterogeneous degrees, we implemented a link update dynamics where links of the network are selected uniformly at random. Then, one of the two linked nodes copies the state of its neighbor with a certain probability tuned by the influence of its clan. Next, we introduce a distance $d_{i,\nu_i} = |s_i - s_{\nu_i}| \in [0, 2]$ between the opinion s_i of node i and that of its clan ν_i , which weights the probability of node i adopting the state of its neighbor j ,

$$P_{i \rightarrow j} = \frac{1}{1 + e^{\frac{1}{\lambda}(1-d_{i,\nu_i})}}. \quad (1)$$

The opinion of clan ν_i , to which node i belongs, is continuous in $[-1, 1]$ and given by the average $s_{\nu_i} = \sum_{l \neq i} s_l / (r - 1)$, $l \in \nu_i$, where node i is excluded and r indicates the total number of nodes in the group. Parameter $\lambda \in [0, \infty)$ controls the strength of the clan influence, which decreases as λ increases. The probability in Eq. (1) reflects the tendency of individuals to refrain from adopting behaviours that contradict their group norm. Its Fermi-like functional form is a popular updating protocol in evolutionary game theory and is in line with the observed stochasticity in real-world human decision-making processes [16]. The probability is symmetric around $d_{i,\nu_i} = 1$, so that a node that is very aligned with its environment ($d_{i,\nu_i} \rightarrow 0$) has less probability of copying a random neighbor, while the probability increases when the node is not aligned with the opinion of its own clan ($d_{i,\nu_i} \rightarrow 2$). When $\lambda \rightarrow 0$, Eq. (1) tends to a step-function, which leads the system to frozen disordered states. In the limit $\lambda \rightarrow \infty$, the MVM becomes the VM with a rescaled activation

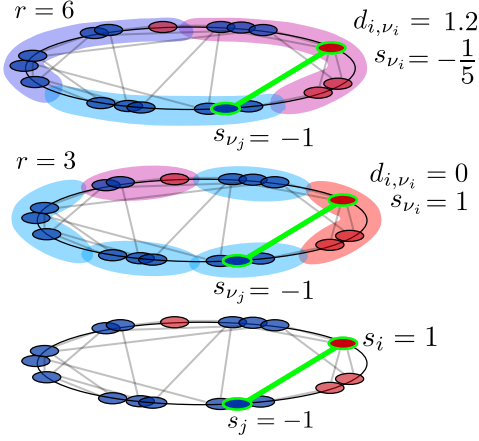


Figure 1. **Illustration of the MVM model.** In the network at the bottom, the link between a copycat node i with opinion $s_i = 1$ and its neighbor j with opposite opinion $s_j = -1$ is highlighted in green. Similarity clans in the middle ($r = 3$) and upper ($r = 6$) layers are colored according to their opinion, ranging from -1 (all nodes blue) to 1 (all red) going through mixed composition (purple). In the middle layer, node i is completely aligned with the opinion of its clan ν_i , so that when $r = 3$ the probability to copy j is low. For clans of size $r = 6$ at the top, the distance in opinion between node i and its clan increases and so does the probability to copy j .

rate that slows the dynamics but eventually leads to consensus. The case with $0 < \lambda < \infty$ is akin to introducing heterogeneous and dynamic activation rates dependant upon the states of nodes and their clans, and leads to competition between metastable opinion domains.

We defined clans as groups of similar nodes detected in network embeddings. To generate the embeddings, we used the tool Mercator [17] which produces a representation of a network in the hyperbolic plane. These embeddings are based on the geometric S^1 model [18], where every node i has a popularity-similarity pair of coordinates (κ_i, θ_i) . Coordinate κ_i is proportional to the node's degree and can be mapped into a radial coordinate r_i in the hyperbolic disc – where nodes with larger degrees lie closer to the center. The angular coordinate θ_i designates the node position in a circle where two nodes are more similar to each other when they have a shorter angular separation $\Delta\theta_{ij}$. In the S^1 model, links between nodes are more probable when nodes are either similar or the product of their κ 's is high.

Given the embedding of a network, clans are constructed by dividing the similarity circle in angular sectors containing r consecutive nodes (see Fig. 1). This is a coarse-graining procedure at the core of the geometric renormalization group [19], which unfolds a network into a self-similar shell of layers with decreasing resolution for increasing r . This means the size

r of the similarity clans (SC) allows us to control for observation scale. We also made groups at random (RG) in order to provide a null model to gauge unexpected behaviour. In addition, groups were based on communities (CG) detected in the geometric maps [20, 21], see Supplemental Material (SM).

We simulated the MVM dynamics in real and synthetic networks, starting from a random uniform distribution of states with an initial density $\rho(t_0) = 0.5$ of nodes in state $s = 1$. For a randomly picked link, the algorithm selects with equal probability a node i , who then adopts the opinion of node j at the other end with $P_{i \rightarrow j}$ given by Eq. (1). At each simulation step, time is advanced by $\Delta t = (1/E)$, where E is the number of links in the network. Despite finite size effects will eventually lead the dynamics to an absorbing consensus state, some realizations can be extremely long-lived. Hence, we set a cutoff time t_c , see Tab. S1 in SM. We measured the level of consensus in the network $\langle \text{Cons} \rangle = \langle |\rho(t_c) - 0.5|/0.5 \rangle$, where the average is over independent realizations, and computed the fluctuations $\chi = (\langle \text{Cons}^2 \rangle - \langle \text{Cons} \rangle^2) / \langle \text{Cons} \rangle$, where we chose the normalization factor following Ref. [22]. Finally, we also evaluated the survival probability S , measuring the fraction of realizations that did not reach consensus at t_c , to elucidate how individual realizations contribute to the average level of consensus.

We considered four data sets from different domains where clans find a natural interpretation: a New Zealand Members of Parliament political network [23] (NZ-MPs), a Facebook friendship network [24] (Facebook), a social proximity network of bottlenose dolphins [25] (Dolphins), and the World Trade Web (WTW) [21]. Results for the four real networks are qualitatively similar, NZ-MPs and WTW are shown in Fig. 2, and Facebook and Dolphins in Figs. S1-S2. In Fig. 2(a)-(b), we show consensus heatmaps in the (λ, r) configuration space for the MVM dynamics using similarity groups SC, and the control case of random groups RG in Fig. 2(c)-(d). For comparability, r_{\max} is chosen as the group size that divides a network in two portions of $N/2$. The heatmaps show areas of low, moderate and high levels of final agreement, with intermediate consensus values more predominant within $\lambda \in [0.15 - 0.5]$ as r grows. In contrast, for smaller clans $r \lesssim 20$, intermediate levels of consensus are more difficult to sustain in all real networks, specially in the region $\lambda \in [0.25 - 0.30]$. This indicates that clan influence at smaller scales dictates more drastically whether the system evolves towards global agreement or not. Furthermore, when groups are random, all real networks display a neat transition centered at $\lambda_{\text{crit}} \approx 0.15$ independent of scale r , see also Fig. S1. This means that mixed opinion configurations are invariably less

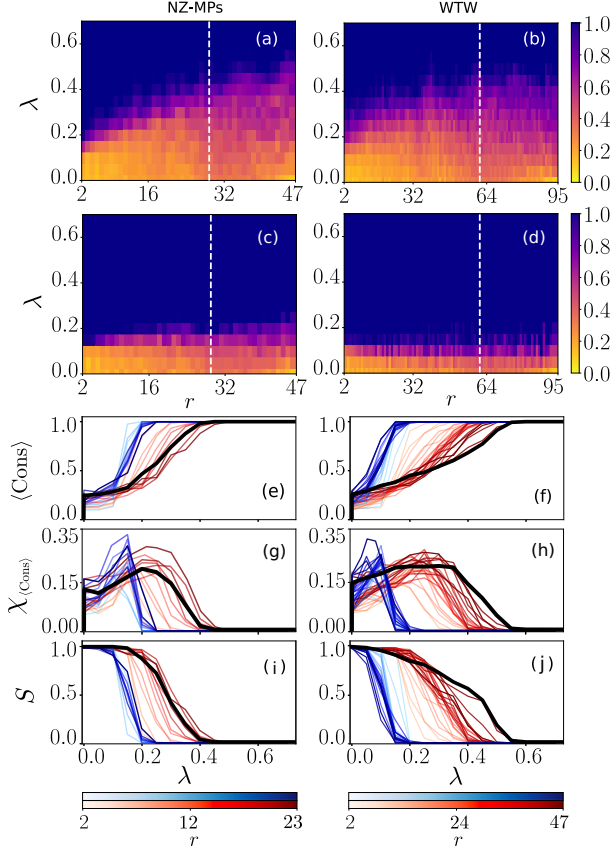


Figure 2. **MVM consensus in real networks.** Consensus heatmaps using SC (a)-(b) and RG (c)-(d) over 100 realizations. Parameter space confined in $r \in [2, N/4]$ and $\lambda \in [10^{-5}, 0.7]$. A white dashed line across the heatmap denotes the size r_c of the largest community detected via the CGM. In plots (e)-(j) red curves correspond to SC and blue ones to RG. Darker tones indicate larger group sizes in both cases. Solid black lines denote groups corresponding to communities. Average consensus $\langle \text{Cons} \rangle$ (e)-(f), fluctuations of average consensus level (g)-(h), and survival probability (i)-(j) against strength of group-influence λ for several group sizes r .

stable over time when groups do not capture actual similarities.

In Fig. 2(e)-(f), we show a projection of the level of consensus against λ . All networks show a more abrupt transition for RG than for SC, and SC slopes show significant variation with r . The fluctuations χ in Fig. 2(g)-(h) show maxima around $\lambda_{\text{crit}}(r) < 0.2$ for RG, while for SC peaks appear at higher values $\lambda_{\text{crit}}(r) > 0.2$ and present lower maxima in all cases. The survival probability S at the bottom of Fig. 2, shows a decreasing trend with λ which demonstrates agreement is more easily achieved as group influence is dissolved. However, the decay is more abrupt for RG curves, which indicates that at $\lambda_{\text{crit}}(r)$ the networks are in very low agreement configurations, but as soon as $\lambda > \lambda_{\text{crit}}(r)$ most runs reach full consensus

before the simulation cutoff time. Simulations with smaller r in Fig. 2(i)-(j) decay fast and continuously to 0 while the process is slower and less monotonous for larger values of r , see Fig. S3. Besides, compared to RG, SC curves show less overlap and are shifted towards larger values of λ , indicating a more progressive transition to consensus demanding more freedom from the group influence.

Finally, we simulated the MVM dynamics using groups corresponding to geometric communities detected via the Critical Gap Method [21]. Hyperbolic embeddings of real networks present angular distributions where high concentrations of nodes in certain angular regions reveal meaningful groups of different sizes made of affine nodes. Results of running the MVM dynamics for CG are reported using black solid lines on Fig. 2(e)-(j) and Figs. S2-S3. Interestingly, when examining $\langle \text{Cons} \rangle$, χ , and S , we identify a pattern that holds across networks despite their different nature, number of communities n_c , and size of the largest community r_c (see Table S1). This is, the results for CG follow approximately the trend of the results for SC curves of $r = r_c$. This means that the largest community of the network effectively is effectively ruling the evolution and eventual outcome of the MVM dynamics.

Simulations on \mathbb{S}^1 synthetic networks allowed us to corroborate these results and estimate the impact of specific topological features in the final stage of the dynamics. We generated \mathbb{S}^1 synthetic networks of sizes $N = 1000, 5000$ nodes and realistic parameters γ and β , that control the scale-freeness of the degree distribution and the mean clustering coefficient, respectively. Consensus heatmaps, fluctuations, and the survival probability are shown in Fig. S4. As observed for real networks, SC clans undergo a progressive transition from low to high consensus within a range of λ values particular of each network and dependant on the group scale r , while RG groups exhibit a sharp transition localized at $\lambda_{\text{crit}} \lesssim 0.15$ with unanimity dominating the majority of the phase space. We confirm that a minor increase in λ for small SC clans can lessen the strength of group influence enough to suddenly push the system towards fast consensus as happens with RG. Oppositely, for larger SC clans a higher rate of opinion exchange allows to sustain more intermediate levels of global consensus for a wider range of λ , see Fig. S4(g)-(h). In summary, we validated the results obtained for real networks and found that unanimity is usually harder to achieve as network topology becomes more homogeneous and clustered (increasing γ and β), see Figs. S5-S6.

Following, we show that similarity clans in the MVM dynamics trigger the formation of metastable clusters of homogeneous opinion in similarity space, which prevent rapid collapse into consensus.

Fig. 3(a)-(b) show the evolution of the average density $\langle \rho \rangle$ of nodes in state $s = 1$ in equally sized angular bins for the NZ-MPs and WTW, respectively. Initially, two opinions, $s = \{-1, 1\}$, were homogeneously spread across the similarity space of both networks. As time passed, $\langle \rho \rangle$ increased in the NZ-MPs on a wide region (red area), while the opposite opinion (blue) prevailed in the remaining angular space. For the WTW, two clusters of $s = 1$ – notice continuous boundary conditions – remained for most of the simulation separated by two other clusters of opposite opinion $s = -1$, which eventually joined ends making $\langle \rho \rangle = 0$. See also the evolution of the average group opinion over time for similarity groups in Fig. S7.

In SM Fig. S8, we report WTW results for various clan sizes r while fixing $\lambda = 0.6$. We observe opposite opinions tend to develop in separate angular regions independently of r , until one colonizes the space of the other or a big fluctuation drives the system to sudden full consensus. In general, it is difficult to detect more than one angular domain per opinion such as displayed in Fig. 3(b). Besides, we fixed the group size to $r = 10$ for both datasets, expanded the range of λ values used to simulate the evolution of $\langle \rho \rangle$ and compared SC and RG prescriptions in Figs. S9-S10. Importantly, we found that random groups do not sustain geometric domains over time. Instead, a higher or lower $\langle \rho \rangle$ may alternate at times but always spreading homogeneously across all angular bins. Besides, all RG simulations last significantly shorter on average than the ones with similarity clans. We, thus, confirm that similarity between nodes is key to support metastable opinion clusters.

In Figs. 3(c)-(d), the hyperbolic maps showcase the spatial distribution of opinions in network snapshots for a single realization of the dynamics. Akin to domain formation in lattice topologies, we visualize the emergence of clusters of homogeneous opinion along the angular dimension of the hyperbolic disc. Furthermore, we provide two animations comparing the MVM temporal evolution of node states in the hyperbolic maps of the WTW, under SC and RG respectively [26]. The animation for SC clearly features two spatial clusters that are sustained over time. We note also that nodes alternating state most frequently are positioned at the borders of the two adjoining opinion domains. On the contrary, the animation using RG does not exhibit any opinion segregation of node states along the circle. In this case, the dynamics evolves over time without nodes being more active in any particular region of the angular space.

We have shown that MVM dynamics on real and synthetic networks can reach mixed binary opinions or full consensus depending on the scale of the groups and on the strength of their influence. Specifically, larger similarity clans can sustain for longer mixed

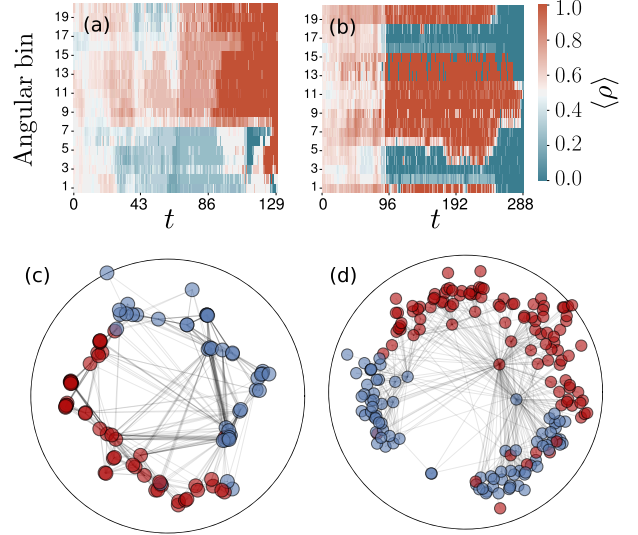


Figure 3. **Geometric opinion domains** of the NZ-MPs (left column) and the WTW (right column) networks. (a)-(b) Time evolution of average density of nodes in state $s = 1$ ($\langle \rho \rangle$) in 20 equally sized bins of the angular coordinate θ ($r = 10$, $\lambda = 0.45$). (c)-(d) Hyperbolic maps of a snapshot of the MVM dynamics using SC ($r = 10$, $\lambda = 0.45$). Two angular domains of different opinion are visible. Red for state $s = 1$ and blue for state $s = -1$.

opinion configurations while a large number of small clans yields a more abrupt transition between very low and very high levels of consensus as group influence diminishes. This behavior is also found for random groups of any size. More diversity can, thus, be achieved either by mixing or partitioning the groups, which helps explain why we don't observe that big structured populations easily come to a full consensus in the real world.

Beyond group scale and strength of influence, group composition radically affects the outcome of MVM opinion dynamics. Although large differences in backgrounds and perspectives might be expected to contribute to gridlock, we did not find this to be the case. We found that the dynamics typically survived longer without reaching global agreement when groups consisted of affine nodes. This is due to the formation of metastable domains of same opinion, which create visible spatial patterns in the angular dimension of the hyperbolic maps of networks. On the contrary, when groups were randomized the opposite was true. This indicates that group diversity can help promote global agreement by reducing friction between sectors of like-minded individuals that pull in opposite directions. Indeed, real observations support the ability of diverse interdisciplinary teams to operate smoothly [27].

Our multiscale framework can be exported to other dynamical processes where scale and group influence

may have a role. For instance, to understand how social acceptance is modified depending on the backup tribe of the influencer. Another possibility is to include multiscale zealots to mimic political parties with stringent ideologies, or add multiple discrete opinions. At the same time, a complete characterization of the MVM model, including the nature of the observed transition and the existence of conserved quantities, would be interesting and remains for future work.

We thank Alex Arcas for a preliminar related exploratory study and Marián Boguñá for helpful comments. We acknowledge support from the Agencia Estatal de Investigación of Spain project number PID2019-106290GB-C22/AEI/10.13039/501100011033.

* marian.serrano@ub.edu

- [1] Suchecki, K., Eguíluz, V. M. & Miguel, M. S. Voter model dynamics in complex networks: Role of dimensionality, disorder, and degree distribution. *Physical Review E* **72**, 036132 (2005).
- [2] Castellano, C., Fortunato, S. & Loreto, V. Statistical physics of social dynamics. *Reviews of modern physics* **81**, 591 (2009).
- [3] Castellano, C., Vilone, D. & Vespignani, A. Incomplete ordering of the voter model on small-world networks. *EPL* **63**, 153 (2003).
- [4] Vilone, D. & Castellano, C. Solution of voter model dynamics on annealed small-world networks. *Phys Rev E* **69**, 016109 (2004).
- [5] Sood, V., Antal, T. & Redner, S. Voter models on heterogeneous networks. *Phys Rev E* **77**, 041121 (2008).
- [6] Redner, S. Reality-inspired voter models: A mini-review. *Comptes Rendus Physique* **20**, 275–292 (2019).
- [7] Baumann, F., Lorenz-Spreen, P., Sokolov, I. & Starnini, M. Modeling echo chambers and polarization dynamics in social networks. *Phys Rev Lett* **124**, 048301 (2020).
- [8] Hobson, E., Mønster, D. & DeDeo, S. Aggression heuristics underlie animal dominance hierarchies and provide evidence of group-level social information. *PNAS* **9**, 118 (2021).
- [9] Castellano, C., Muñoz, M. A. & Pastor-Satorras, R. Nonlinear q -voter model. *Phys. Rev. E* **80**, 041129 (2009).
- [10] Vilela, A. L. *et al.* Three-state majority-vote model on scale-free networks and the unitary relation for critical exponents. *Scientific Reports* **10**, 1–11 (2020).
- [11] Peralta, A. F., Carro, A., San Miguel, M. & Toral, R. Analytical and numerical study of the non-linear noisy voter model on complex networks. *Chaos: An Interdisciplinary Journal of Nonlinear Science* **28**, 075516 (2018).
- [12] Diakonova, M., Nicosia, V., Latora, V. & San-Miguel, M. Irreducibility of multilayer network dynamics: the case of the voter model. *New J Phys* **18**, 023010 (2016).
- [13] Amato, N., R. Kouvaris, San-Miguel, M. & Díaz-Guilera, A. Opinion competition dynamics on multiplex networks. *New J Phys* **19**, 123019 (2017).
- [14] Tsarev, D., Trofimova, A., Alodjants, A. & Khrennikov, A. Phase transitions, collective emotions and decision-making problem in heterogeneous social systems. *Sci Rep* **9**, 18039 (2019).
- [15] Boguñá, M. *et al.* Network geometry. *Nature Reviews Physics* **3**, 114–135 (2021).
- [16] Matjaž, P. Phase transitions in models of human cooperation. *Phys Lett A* **380**, 2803–2808 (2016).
- [17] García-Pérez, G., Allard, A., Serrano, M. & Boguñá, M. Mercator: uncovering faithful hyperbolic embeddings of complex networks. *New J Phys* **21**, 123033 (2019).
- [18] Serrano, M. Á., Krioukov, D. & Boguñá, M. Self-similarity of complex networks and hidden metric spaces. *Phys Rev Lett* **100**, 078701 (2008).
- [19] García-Pérez, G., Boguñá, M. & Serrano, M. Á. Multiscale unfolding of real networks by geometric renormalization. *Nature Physics* **14**, 583–589 (2018).
- [20] Serrano, M. Á., Boguñá, M. & Sagues, F. Uncovering the hidden geometry behind metabolic networks. *Mol. BioSyst.* **8**, 843–850 (2012).
- [21] García-Pérez, G., Boguñá, A. M., Allard & Serrano, M. Á. The hidden hyperbolic geometry of international trade: World trade atlas 1870–2013. *Sci. Rep.* **6**, 33441 (2016).
- [22] Colomer-de Simón, P. & Boguñá, M. Double percolation phase transition in clustered complex networks. *PRX* **4**, 041020 (2014).
- [23] Curran, B., Higham, K., Ortiz, E. & Vasques-Filho, D. Look who’s talking: Two-mode networks as representations of a topic model of new zealand parliamentary speeches. *PloS one* **13**, e0199072 (2018).
- [24] Traud, A., Kelsic, E., Mucha, P. & Porter, M. Comparing community structure to characteristics in on-line collegiate social networks. *SIAM Rev.* **53**, 526–543 (2011).
- [25] Gazda, S., Iyer, S., Killingback, T., Connor, R. & Brault, S. The importance of delineating networks by activity type in bottlenose dolphins (*tursiops truncatus*) in cedar key, florida. *R Soc Open Sci* **2**, 140263 (2015).
- [26] Ortiz, E. Github: Multiscale-voter-model. <https://github.com/elisendaortiz/Multiscale-Voter-Model> (2021).
- [27] Balagna, J. *et al.* Consensus-driven approach for decision-making in diverse groups. *AJPH* **110**, 5 (2020).